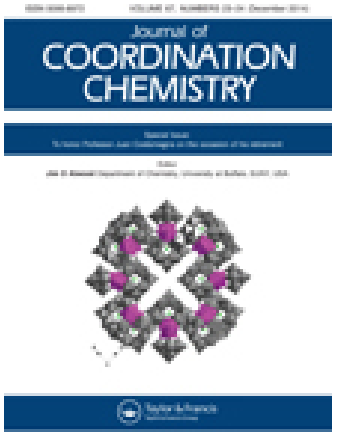

Journal of Coordination Chemistry
Publication details, including instructions for authors and subscription information:
http://www.tandfonline.com/loi/gcoo20

Influence of supporting ligand microenvironment on the aqueous stability and visible light-induced CO-release reactivity of zinc flavonolato species

Stacey N. Anderson[a], Mark Noble[a], Katarzyna Grubel[a], Brooks Marshall[a], Atta M. Arif[b] & Lisa M. Berreau[a]

[a] Department of Chemistry and Biochemistry, Utah State University, Logan, UT, USA

[b] Department of Chemistry, University of Utah, Salt Lake City, UT, USA

Accepted author version posted online: 21 Oct 2014.Published online: 14 Nov 2014.

To cite this article: Stacey N. Anderson, Mark Noble, Katarzyna Grubel, Brooks Marshall, Atta M. Arif & Lisa M. Berreau (2014) Influence of supporting ligand microenvironment on the aqueous stability and visible light-induced CO-release reactivity of zinc flavonolato species, Journal of Coordination Chemistry, 67:23-24, 4061-4075, DOI: 10.1080/00958972.2014.977272

To link to this article: http://dx.doi.org/10.1080/00958972.2014.977272

Journal of Coordination Chemistry, 2014
Vol. 67, Nos. 23–24, 4061–4075, http://dx.doi.org/10.1080/00958972.2014.977272

Influence of supporting ligand microenvironment on the aqueous stability and visible light-induced CO-release reactivity of zinc flavonolato species

STACEY N. ANDERSON†, MARK NOBLE†, KATARZYNA GRUBEL†, BROOKS MARSHALL†, ATTA M. ARIF‡ and LISA M. BERREAU*†

†Department of Chemistry and Biochemistry, Utah State University, Logan, UT, USA
‡Department of Chemistry, University of Utah, Salt Lake City, UT, USA

(*Received 1 September 2014; accepted 13 October 2014*)

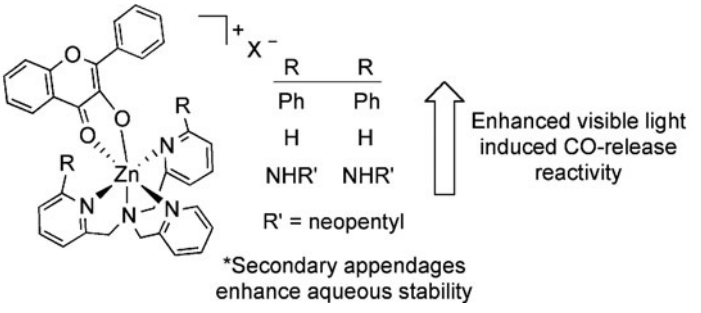

The visible light-induced CO-release reactivity of the zinc flavonolato complex [(6-Ph_2TPA)Zn(3-Hfl)]ClO_4 (**1**) has been investigated in 1 : 1 H_2O : DMSO. Additionally, the effect of ligand secondary microenvironment on the aqueous stability and visible light-induced CO-release reactivity of zinc flavonolato species has been evaluated through the preparation, characterization, and examination of the photochemistry of compounds supported by chelate ligands with differing secondary appendages, [(TPA)Zn(3-Hfl)]ClO_4 (**3**; TPA = tris-2-(pyridylmethyl)amine) and [(bnpapa)Zn(3-Hfl)]ClO_4 (**4**; bnpapa = *N*,*N*-bis((6-neopentylamino-2-pyridyl)methyl)-*N*-((2-pyridyl)methyl)amine)). Compound **3** undergoes reaction in 1 : 1 H_2O : DMSO resulting in the release of the free neutral flavonol. Irradiation of acetonitrile solutions of **3** and **4** at 419 nm under aerobic conditions results in quantitative, photoinduced CO-release. However, the reaction quantum yields under these conditions are lower than that exhibited by **1**, with **4** exhibiting an especially low quantum yield. Overall, the results of this study indicate that positioning a zinc flavonolato moiety within a hydrophobic microenvironment is an important design strategy toward further developing such compounds as CO-release agents for use in biological systems.

Keywords: Zinc; Microenvironment; Photochemistry; Carbon monoxide; Hydrogen bonding

*Corresponding author. Email: lisa.berreau@usu.edu

1. Introduction

The development of carbon monoxide-releasing molecules (CORMs) for use in biological systems is of significant current interest [1–7]. This is due to the identification of several beneficial health effects associated with the controlled administration of small amounts of CO. These include anti-inflammatory and antiapoptotic effects, as well as the promotion of vasodilation and protection of tissues against reperfusion injury [4]. To date, the vast majority of CORMs reported are low-valent metal carbonyl compounds. These compounds, while exhibiting a number of favorable properties for biological use, also have limitations, including the fact that many cannot be controlled in terms of the location and timing of the CO-release. In this regard, metal carbonyl-based CORMs that exhibit photoinduced CO-release reactivity (photoCORMs) using low-energy visible light are of particular current interest [1, 2, 8–13]. However, an important unresolved issue for these compounds is the potential for toxicity resulting from the remaining metal/ligand fragment following CO-release.

We are interested in developing new types of photoinduced CO-releasing molecules that are not based on the metal-carbonyl unit. In this regard, it is known that quercetin dioxygenases (QDOs) catalyze the oxidative breakdown of flavonols to give CO and an *O*-benzoylsalicylic acid (*O*-bs) derivative as products [14]. In studies of synthetic complexes of relevance to the enzyme/substrate adducts of QDOs, we discovered stoichiometric, UV light-induced CO-release reactivity for a family of divalent metal complexes ([(6-Ph_2TPA)M(3-Hfl)]X, M = Zn(II), Co(II) Cu(II), Ni(II), Mn(II); X = ClO_4^- or OTf^-) containing a deprotonated 3-hydroxy-4-flavonolato ligand (3-Hfl) and supported by a tetradentate N_4-donor chelate ligand (6-Ph_2TPA, *N*,*N*-bis((6-phenyl-2-pyridyl)methyl)-*N*-((2-pyridyl)methyl) amine) [15, 16]. For these complexes, CO-release occurs via a photoinduced, dioxygenase-type reaction akin to the thermal reaction catalyzed by QDOs. The reaction observed for [(6-Ph_2TPA)Zn(3-Hfl)]ClO_4 (**1**) in CH_3CN under O_2 is shown in scheme 1. The quantum yield for this reaction with irradiation at 300 nm (ϕ = 0.09(1)) [16] is an order of magnitude higher than that exhibited by structurally similar Mn(II), Co(II), Ni(II), Cu(II) complexes (ϕ = 0.005–0.008) [16]. This is the result of quenching of the excited state in the complexes containing an open-shell d^n metal ion. The photoinduced reaction pathway for O_2-dependent CO-release from [(6-Ph_2TPA)Zn(3-Hfl)]ClO_4 (**1**) likely involves either the coordinated flavonolato ligand acting as a photosensitizer to generate singlet oxygen ($^1O_2$), which can then react with ground state **1**, or an excited state singlet to triplet conversion of the zinc-bound flavonolato anion, which may then undergo reaction with $^3O_2$.

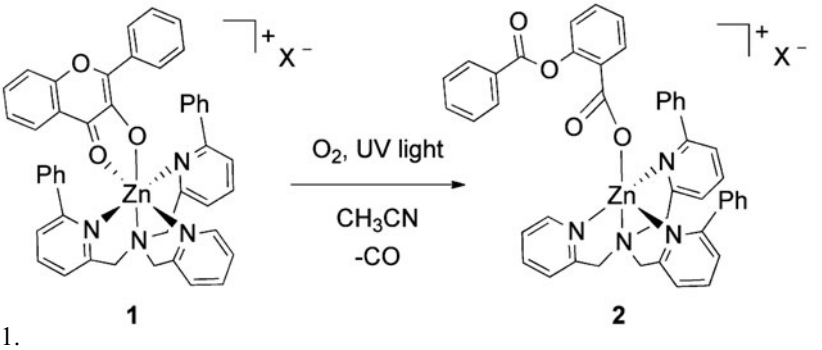

Scheme 1.

The initial studies outlined above have led us to further examine the chemistry of zinc flavonolato species. In the results described herein, we have evaluated the visible light-induced CO-release reactivity of **1** in 1 : 1 H_2O : DMSO. Additionally, we have evaluated how the nature of the supporting chelate ligand, particularly with respect to the secondary microenvironment surrounding the zinc flavonolato moiety, influences the aqueous stability and visible light-induced CO-release reactivity of this unit. These combined results provide evidence that maintaining a hydrophobic microenvironment surrounding the zinc flavonolato moiety is key toward further developing such compounds for use in biological systems.

2. Experimental

2.1. *Chemicals and reagents*

All chemicals and reagents were obtained from commercial sources and used as received unless otherwise noted. Anaerobic procedures were performed under N_2 in either a VAC Atmospheres or an MBRAUN Unilab glovebox. Solvents for glovebox use were dried according to published methods and distilled under N_2 [17]. The preparation of the chelate ligands tris(2-pyridylmethyl)amine (TPA) [18] and *N*,*N*-bis((6-neopentylamino-2-pyridyl) methyl)-*N*-((2-pyridyl)methyl)amine (bnpapa) [19] was accomplished as previously reported. [(6-Ph_2TPA)Zn(3-Hfl)]ClO_4 (**1**) was prepared as previously described [20].

2.2. *Physical methods*

^{1}H NMR spectra were collected using a JEOL ECX-300 or Bruker ARX-400 spectrometer. Chemical shifts (in ppm) are referenced to the residual solvent peaks in CD_2HCN (^{1}H: 1.94 (quintet) ppm). *J* values are given in Hz. IR spectra were recorded on a Shimadzu FTIR-8400 spectrometer as KBr pellets. UV–vis spectra were recorded at ambient temperature using a Hewlett-Packard 8453A diode array spectrophotometer. Emission spectra were collected using a Shimadzu RF-5301PC spectrofluorophotometer using a slit width of 4 nm with the excitation wavelength corresponding to the absorption maximum of the complex above 400 nm. A Rayonet photoreactor equipped with RPR-4190A lamps was used for all photochemical reactions. Quantum yields were determined using potassium ferrioxalate actinometry as a standard to measure photon flux [21–23]. Carbon monoxide was quantified as previously described [16]. Mass spectral data were collected at the Mass Spectrometry Facility, University of California, Riverside. Elemental analyses were performed by Atlantic Microlab, Inc., Norcross, GA using a PE2400 automatic analyzer.

Caution! Perchlorate salts of metal complexes with organic ligands are potentially explosive. Only small amounts should be prepared, and these should be handled with great care [24].

2.3. *Photoreactivity of 1 in 1 : 1 H_2O : DMSO using visible light*

A solution of **1** (0.1 mM in 10 mL 1 : 1 H_2O : DMSO) was placed in a 100-mL round-bottom flask under air. This solution was irradiated at 419 nm until the reaction was determined to be complete as evidenced by loss of the 420-nm absorption band. CO-release was determined to be quantitative by GC. Performing the same reaction in 1 : 1 D_2O : d_6-DMSO confirmed the formation of **2** via comparison of the ^{1}H NMR features with those previously reported for this compound [15].

2.4. *Preparation of zinc flavonolato complexes*

2.4.1. [(TPA)Zn(3-Hfl)]ClO_4 (3). Under a N_2 atmosphere, a methanol solution (2 mL) of $Zn(ClO_4)_2{\cdot}6H_2O$ (40 mg, 0.11 mM) was added to solid TPA (39 mg, 0.13 mM) and the solution was stirred until the chelate ligand had dissolved. The resulting mixture was combined with a methanol solution (2 mL) containing 3-hydroxyflavone (32 mg, 0.13 mM) and $Me_4NOH{\cdot}5H_2O$ (24 mg, 0.13 mM). This mixture was stirred for 4 h at ambient temperature. The solvent was then removed under reduced pressure and the residual solid dissolved in CH_2Cl_2. The CH_2Cl_2 solution was filtered through a celite/glass wool plug, and the product was precipitated via the addition of excess hexanes (40 mL). The isolated solid was dried under reduced pressure. Recrystallization via Et_2O diffusion into CH_3CN yielded yellow crystals suitable for X-ray crystallography (74 mg, 80%). Anal. Calcd for $C_{33}H_{27}ClN_4O_7Zn$ (%): C, 57.24; H, 3.93; N, 8.09. Found: C, 57.55; H, 4.00; N, 7.84. ^{1}H NMR (CD_3CN, 300 MHz) δ 8.9 (br, 2H), 8.80–8.45 (br, 4H), 8.03–7.77 (br, 3H) 7.76–7.59 (m, 4H), 7.58–7.20 (m, 8H), 4.79–4.02 (bs, 6H) ppm; UV–vis (CH_3CN), nm (ε, M^{-1} cm^{-1}) 415 (19,000), 313 (7600); FTIR (KBr, cm^{-1}) 1558 ($\nu_{C=O}$), 1088 (ν_{ClO4}), 619 (ν_{ClO4}); MALDI-MS, *m/z* (relative intensity) $C_{33}H_{27}N_4O_3Zn$: Calcd: 591.1369; Found: 591.1385 ($[M\text{-}ClO_4]^+$, 100).

2.4.2. [(bnpapa)Zn(3-Hfl)]ClO_4 (4). Prepared using a synthetic procedure similar to that employed for the preparation of $[(6\text{-}Ph_2TPA)Zn(3\text{-}Hfl)]ClO_4$ [20]. Recrystallization of the crude product via slow Et_2O diffusion into $CHCl_3$ yielded yellow crystals suitable for single crystal X-ray crystallography (87 mg, 75%). Anal. Calcd for $C_{43}H_{49}ClN_6O_7Zn$(%): C, 59.86; H, 5.72; N, 9.74. Found: C, 60.05; H, 6.02; N, 9.38. ^{1}H NMR (CD_3CN, 300 mHz) δ 8.87 (br, 2H, N–H), 8.73 (d, J = 7.9 Hz, 1H), 8.10 (d, J = 7.9 Hz, 1H), 7.82–7.63 (m, 5H), 7.61–7.52 (m, 2H), 7.50–7.32 (m, 4H), 7.30–7.18 (m, 2H), 6.49 (d, J = 7.2 Hz, 2H), 6.36 (d, J = 8.6 Hz, 2H), 4.52 (d, J = 14.3 Hz, 2H), 4.31 (s, 2H), 4.23 (d, J = 14.3 Hz, 2H), 2.87 (d, J = 7.2 Hz, 1H), 2.83 (d, J = 7.5 Hz, 1H), 2.62 - 2.48 (m, 2H), 0.63 (s, 18H) ppm; UV–vis (CH_3CN), nm (ε, M^{-1} cm^{-1}) 401 (16,500), 321 (18,400); FTIR (KBr, cm^{-1}) 3307 (br, ν_{N-H}), 1560 ($\nu_{C=O}$), 1085 (ν_{ClO4}), 620 (ν_{ClO4}); MALDI-MS, *m/z* (relative intensity) $C_{43}H_{49}N_6O_3Zn$: Calcd: 761.3152; Found: 761.3120 ($[M\text{-}ClO_4]^+$, 100).

2.5. *Photoreactivity of [(L)Zn(3-Hfl)]ClO_4 (L = TPA (3) or bnpapa (4))*

2.5.1. Identification of [(L)Zn(*O*-bs)]ClO_4 products (*O*-bs = *O*-benzoylsalicylato). A solution of each complex ($[(L)Zn(3\text{-}Hfl)]ClO_4$ (L = TPA (**3**) or bnpapa (**4**); 0.1 mM in 10 mL CH_3CN) was placed in a 100-mL round-bottom flask under air. Each solution was irradiated at 419 nm until the reaction was determined to be complete as evidenced by loss of the ~400–415-nm absorption band. The solvent was then removed under reduced pressure, and the residual solid was redissolved in a minimal amount of CH_3CN (ca. 2 mL). Addition of excess Et_2O (~20 mL) resulted in the deposition of a beige solid that was dried *in vacuo* to give the reported yields for $[(TPA)Zn(O\text{-}bs)]ClO_4$ (**5**) and $[(bnpapa)Zn(O\text{-}bs)]ClO_4$ (**6**). $^{18}O_2$-labeled samples were prepared by transferring aliquots of $^{18}O_2$ into frozen CH_3CN solutions of **3** and **4** in 100-mL solvent transfer flasks, followed by irradiation and work-up as described above.

2.5.1.1. *[(TPA)Zn(O-bs)]ClO_4 (5).* Yield: 91%. ^{1}H NMR (CD_3CN, 300 MHz) δ 8.74 (s, 3H), 8.02 (td, J_1 = 7.8, J_2 = 1.5, 4H), 7.73–7.23 (m, 14 H), 4.13 (s, 6H) ppm; FTIR (KBr, cm^{-1}) 1761 ($\nu_{C=O}$); $^{18}O_2$ sample: MALDI-MS, *m/z* (relative intensity); $C_{32}H_{27}N_4{}^{16}O_2{}^{18}O_2Zn$: Calcd 599.1403. Found: 599.1407 ($[M\text{-}ClO_4]^+$; 27).

2.5.1.2. *[(bnpapa)Zn(O-bs)]ClO_4 (6).* Yield: 88%. ^{1}H NMR (CD_3CN, 300 MHz) δ 8.57 (s, 1H), 8.19–7.00 (m, 14H), 6.65 (s, 2H), 6.47 (d, J = 6.4 Hz, 2H), 4.06 (s, 2H), 3.81–3.62 (m, 4H), 3.12–2.87 (m, 6H), 0.85 (s, 18H) ppm; FTIR (KBr, cm^{-1}) 1743 ($\nu_{C=O}$); MALDI, *m/z* (relative intensity); $C_{42}H_{49}N_6{}^{16}O_4Zn$: Calcd: 765.3101. Found: 765.3124 ($[M\text{-}ClO_4]^+$, 30). $^{18}O_2$ sample: MALDI-MS, *m/z* (relative intensity); $C_{42}H_{49}N_6{}^{16}O_2{}^{18}O_2Zn$: Calcd 769.3186. Found: 769.3196 ($[M\text{-}ClO_4]^+$, 58).

2.5.2. Dark control reactions. Solutions of **3** and **4** in CD_3CN (~0.02 M) were prepared in air under minimal red light and placed in NMR tubes. Each NMR tube was then covered with foil and irradiated at 419 nm for a specific amount of time (**3** : 24 h; **4** : 96 h). For both, evaluation of the solution by ^{1}H NMR indicated that no reaction had occurred. These results indicate that the CO-release reactions of **3** and **4** are photoinduced and not thermal processes.

2.5.3. Anaerobic control reactions. Solutions of **3** and **4** in CD_3CN (~0.02 M) were prepared under N_2 in a glovebox and placed in NMR tubes. Each NMR tube was then irradiated at 419 nm for a specific amount of time (**3** : 24 h; **4** : 96 h). For both, evaluation of the solution by ^{1}H NMR indicated that no reaction had occurred. These results indicate that the CO-release reactions of **3** and **4** require O_2.

2.6. *X-ray crystallography*

2.6.1. Data collection and refinement. Single crystals of **3·CH_3CN** and **4·$CHCl_3$** were each mounted on a glass fiber using viscous oil and then transferred to a Nonius Kappa CCD diffractometer for data collection using Mo Kα radiation (λ = 0.71073 Å). Methods of unit cell refinement and determination of final cell constants have been previously reported [25]. The data collected for each compound were corrected for Lorentz polarization and absorption effects using DENZO-SMN and SCALEPAC [26]. Each structure was solved using a combination of direct methods and heavy atoms using SIR 97.

2.6.2. Structure solution. Complexes **3·CH_3CN** and **4·$CHCl_3$** crystallize in the space groups *$P2_1/n$* and *P–1*, respectively. All non-hydrogen atoms were refined with anisotropic displacement coefficients. All hydrogen atoms were assigned isotropic displacement coefficients (U(H) = 1.2U(C) or = 1.5U(C_{methyl})), and their coordinates were allowed to ride using SHELXL97 [27]. In **3·CH_3CN,** the perchlorate anion exhibits disorder of three of the oxygen atoms. In **4·$CHCl_3$**, hydrogen-bonding interactions are found between the secondary amine NH units of O(1) of the coordinated flavonolato ligand.

3. Results and discussion

3.1. *Spectroscopic features and photoinduced CO-release reactivity of 1 in 1 : 1 H_2O : DMSO*

3.1.1. Absorption and emission properties. Compound **1** is not soluble in water but exhibits good solubility in 1 : 1 H_2O : DMSO. As shown in figure 1(a), **1** exhibits a ~420-nm absorption band in this solvent mixture which is similar to the spectrum produced in CH_3CN. Evaluation of this solution after 24 h of storage at ambient temperature in the dark revealed no spectral changes. Hence, the compound is stable in an aqueous environment under dark, aerobic conditions.

Excitation into the 420 nm absorption maximum of **1** produces a fluorescent emission at ~480 nm when the compound is dissolved either in CH_3CN or 1 : 1 H_2O : DMSO under anaerobic conditions [figure 1(b)]. The overall intensity of the emission is reduced in the aqueous/organic mixture.

3.1.2. Photoinduced CO-release reactivity of 1 using visible light. Irradiation of **1** in 1 : 1 H_2O : DMSO using visible light (419 nm) under air results in the release of one equivalent of CO (table 1) and the formation of [(6-Ph_2TPA)Zn(*O*-bs)]ClO_4 (**2**). The quantum yield for this reaction ($\phi = 0.006$) is only twofold lower than that observed in acetonitrile under similar conditions.

3.2. *Synthesis and characterization of 3 and 4*

To investigate the influence of the chelate ligand on the aqueous stability and photoinduced CO-release reactivity of **1**, analogs were prepared and characterized using tetradentate chelate ligands that either lacked secondary appendages (TPA) or contained hydrogen-bond donor moieties (bnpapa).

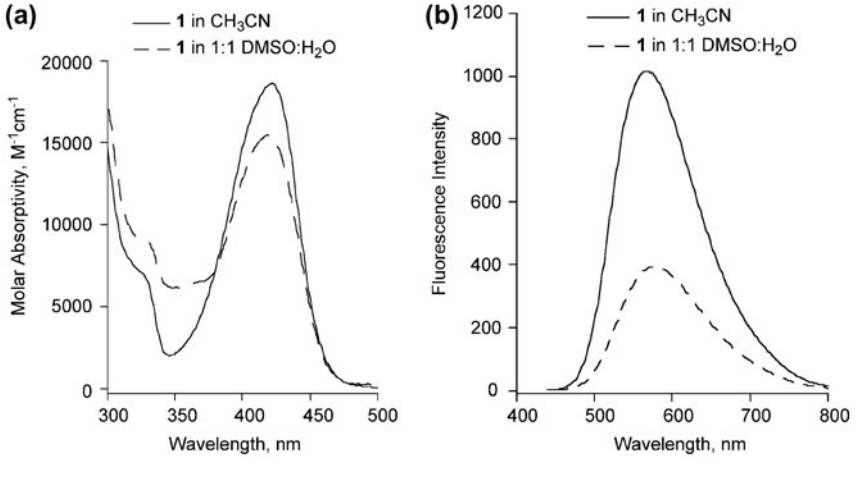

Figure 1. (a) Absorption spectra of **1** in CH_3CN and 1 : 1 DMSO : H_2O. (b) Fluorescence emission spectra of **1** in CH_3CN and 1 : 1 DMSO : H_2O generated upon excitation at 420 nm.

Table 1. Reaction quantum yields and CO quantification for the visible light induced aerobic CO-release reactions of **1**, **3**, and **4**.

Compound	Solvent	$\phi^{a,b}$	Eq. CO[b]
1	CH_3CN	0.012(2)	0.99(2)
	1 : 1 H_2O/DMSO	0.006(1)	0.977(6)
3	CH_3CN	0.0060(9)	0.99(1)
4	CH_3CN	0.000269(8)	1.00(4)

[a]$\lambda_{irr} = 419$ nm.
[b]Average of three independent determinations.

3.2.1. Synthesis. Admixture of the appropriate chelate ligand (TPA or bnpapa) with Zn $(ClO_4)_2 \cdot 6H_2O$, followed by the addition of a solution containing a mixture of 3-hydroxyflavone (3-HflH) and $Me_4NOH \cdot 5H_2O$, respectively, produced yellow reaction mixtures. After workup, each complex was isolated as a crystalline solid (scheme 2) in 75–80% yield. The zinc flavonolato complexes $[(TPA)Zn(3\text{-}Hfl)]ClO_4$ (**3**) and $[(bnpapa)Zn(3\text{-}Hfl)]ClO_4$ (**4**) were characterized by elemental analysis, X-ray crystallography, absorption and emission spectroscopy, IR, ^1H NMR, and mass spectrometry.

3.2.2. Elemental analysis. The elemental analysis data for bulk samples of **3** and **4** are consistent with the dried powder form of each complex having an analytical formulation that lacks the CH_3CN and $CHCl_3$ solvate molecules, respectively, that are found in the X-ray structures of these complexes (vide infra).

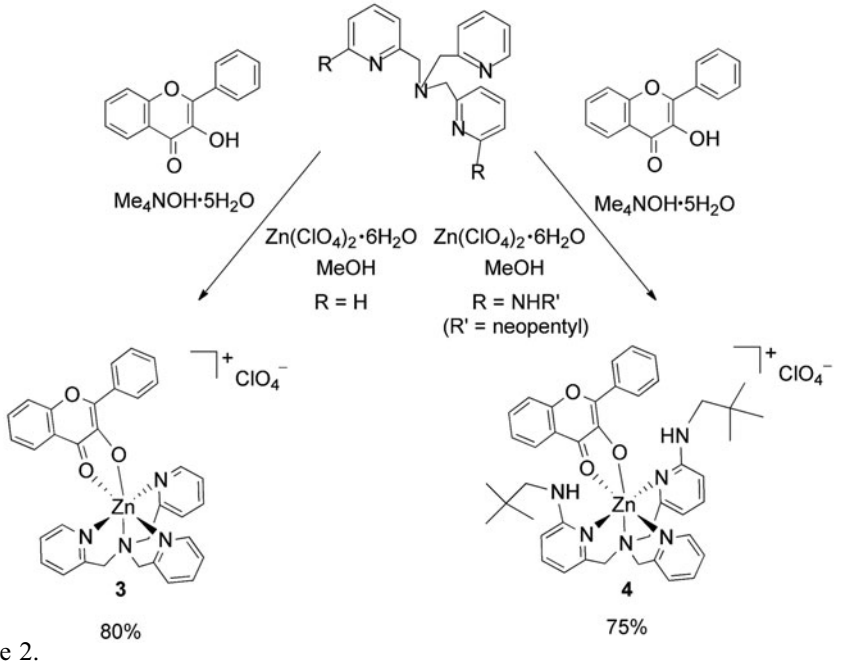

Scheme 2.

3.2.3. X-ray crystallography. Representations of the cationic portions of **3·CH$_3$CN** and **4·CHCl$_3$** are shown in figure 2. Details of the X-ray data collection and refinement are given in table 2. Bond distances and angles within the cationic portions of these structures are given in table 3. The Zn(II) centers in the cationic portions of **3·CH$_3$CN** and **4·CHCl$_3$** have a coordination number of six and exhibit a distorted pseudo-octahedral geometry. This differentiates the solid-state structures of these cations from that found for **1·2CH$_2$Cl$_2$**,

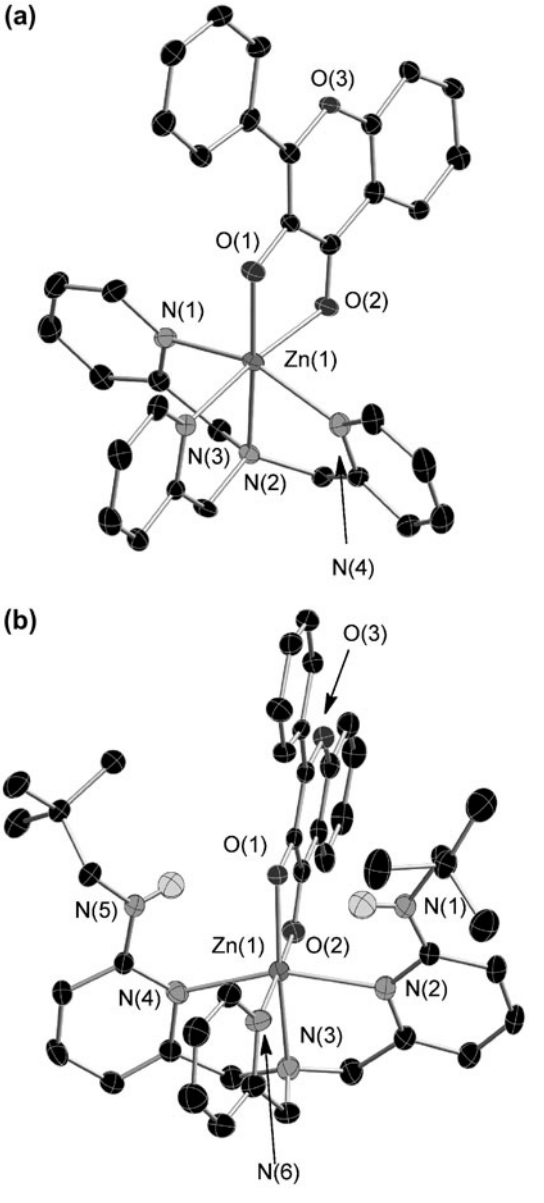

Figure 2. Thermal ellipsoid (50%) representations of the cationic portions of (a) **3** and (b) **4**. Hydrogen atoms except those of the N–H units have been omitted for clarity.

Table 2. Summary of X-ray data collection and refinement.

	3·CH$_3$CN	**4·CHCl$_3$**
Empirical formula	$C_{35}H_{30}ClN_5O_7Zn$	$C_{44}H_{50}Cl_4N_6O_7Zn$
Formula weight	733.46	982.07
Crystal system	Monoclinic	Triclinic
Space group	*P2$_1$/n*	*P–1*
a (Å)	10.7484(2)	11.8486(3)
b (Å)	17.7387(3)	12.4945(4)
x (Å)	17.7291(2)	16.2785(5)
α (°)	90	88.8622(12)
β (°)	105.7229(10)	75.3891(15)
γ (°)	90	81.2326(16)
V (Å^3)	3253.80(9)	2304.29(12)
Z	4	2
Density (Calcd) (Mg m^{-3})	1.497	1.415
Temp (K)	150(1)	150(1)
Crystal size (mm^3)	0.38 × 0.23 × 0.08	0.35 × 0.28 × 0.10
Diffractometer[a]	Nonius Kappa CCD	Nonius Kappa CCD
Abs. coeff. (mm^{-1})	0.896	0.821
2*θ* max (°)	54.96	50.68
Reflections collected	14,263	15,983
Indep. reflections	7433	8410
Variable parameters	443	588
R_1/wR_2[b]	0.0405/0.0962	0.0490/0.1235
Goodness-of-fit (F^2)	1.037	1.027
Largest diff. (e Å^{-3})	0.919; −0.530	1.106; −0.664
CCDC number	1006160	1006159

[a]Radiation used: Mo Kα (λ = 0.71073 Å).
[b]$R_1 = \sum \; | \; |F_o| - |F_c| | / \sum \; |F_o|$; w$R_2 = [\sum[w(F_o^2 - F_c^2)^2]/[\sum(F_o^2)^2]]^{1/2}$ where $w = 1/[\sigma^2(F_o^2) + (aP)^2 + bP]$.

Table 3. Selected bond distances (Å) and angles (°) for **3·CH$_3$CN** and **4·CHCl$_3$**.[a]

3·CH$_3$CN			
Zn(1)–O(1)	1.9834(17)	O(1)–Zn(1)–O(2)	81.57(7)
Zn(1)–O(2)	2.1373(17)	O(1)–Zn(1)–N(3)	103.21(7)
Zn(1)–N(1)	2.186(2)	N(3)–Zn(1)–O(2)	174.39(7)
Zn(1)–N(2)	2.2116(18)	O(1)–Zn(1)–N(4)	108.68(7)
Zn(1)–N(3)	2.1179(19)	N(3)–Zn(1)–N(4)	87.76(7)
Zn(1)–N(4)	2.171(2)	O(2)–Zn(1)–N(4)	87.90(7)
O(1)–C(19)	1.334(3)	O(2)–Zn(1)–N(2)	94.34(6)
O(2)–C(20)	1.249(3)	N(4)–Zn(1)–N(2)	77.13(7)
C(19)–C(20)	1.439(3)	N(1)–Zn(1)–N(2)	76.83(7)
O(1)–Zn(1)–N(2)	172.64(7)	O(1)–Zn(1)–N(1)	97.19(7)
N(3)–Zn(1)–N(2)	81.23(7)	N(3)–Zn(1)–N(1)	89.31(7)
N(4)–Zn(1)–N(1)	153.95(8)	O(2)–Zn(1)–N(1)	93.04(7)
4·CHCl$_3$			
Zn(1)–O(1)	2.020(2)	O(1)–Zn(1)–N(6)	106.46(9)
Zn(1)–O(2)	2.159(2)	O(1)–Zn(1)–N(3)	171.00(10)
Zn(1)–N(2)	2.200(3)	N(6)–Zn(1)–N(3)	82.28(11)
Zn(1)–N(3)	2.144(3)	O(1)–Zn(1)–O(2)	80.24(8)
Zn(1)–N(4)	2.181(3)	N(6)–Zn(1)–O(2)	172.05(9)
Zn(1)–N(6)	2.124(3)	N(3)–Zn(1)–O(2)	91.21(10)
O(1)–C(29)	1.320(4)	N(3)–Zn(1)–N(4)	80.08(10)
O(2)–C(30)	1.254(4)	O(2)–Zn(1)–N(4)	91.51(9)
C(29)–C(30)	1.460(4)	O(1)–Zn(1)–N(2)	99.41(9)
N(6)–Zn(1)–N(2)	95.04(11)	O(1)–Zn(1)–N(4)	102.80(9)
N(3)–Zn(1)–N(2)	77.30(10)	N(6)–Zn(1)–N(4)	82.91(11)
N(4)–Zn(1)–N(2)	157.35(10)	O(2)–Zn(1)–N(4)	91.51(9)

[a]Estimated standard deviations in the last significant figure are given in parentheses.

which exhibits an overall coordination number of five, a distorted square pyramidal geometry (τ = 0.35) [28], and a dissociated phenyl-appended pyridyl donor. All three complexes exhibit bidentate coordination of the flavonolato ligand, with the shorter zinc–oxygen distance in each involving the deprotonated hydroxyl donor (**1·2CH$_2$Cl$_2$**: 1.951(2) Å; **3·CH$_3$CN**: 1.9834(17) Å; **4·CHCl$_3$**: 2.020(2) Å) and a longer bond to the ketone oxygen (**1·2CH$_2$Cl$_2$**: 2.1175(19) Å; **3·CH$_3$CN**: 2.1373(17) Å; **4·CHCl$_3$**: 2.159(2) Å). The $\Delta_{Zn\text{-}O}$ value is similar in this family of compounds, with all being found in the range of 0.14–0.17 Å. Generally, the observed bond lengths and $\Delta_{Zn\text{–}O}$ values for the complexes described herein fall within the ranges of other previously reported zinc flavonolato complexes (1.98–2.24 Å; $\Delta_{Zn\text{–}O}$ = 0.16–0.26 Å) [29–31]. Notably, both Zn–O distances elongate across the supporting chelate ligand series in the order 6-Ph$_2$TPA < TPA < bnpapa. The same trend is found in the average Zn–N$_{py}$ distance, which increases from 2.11 Å in the 6-Ph$_2$TPA-ligated complex to 2.16 and 2.17 Å in the TPA- and bnpapa-ligated complexes, respectively. This latter trend is likely due to the effect of overall coordination number, as well as the presence of the secondary amine donor appendages in the bnpapa-ligated system, which introduces additional steric hindrance.

Examination of the bond lengths within the coordinated flavonolato ligand shows that all three complexes exhibit a similar slight elongation (~0.02 Å) of the ketone carbonyl C–O bond and a slight contraction (~0.02–0.04 Å) of the C–O bond of the hydroxyl donor relative the distances found in the free flavonol (1.232(3) and 1.357(3) Å, respectively) [32]. The C=C bond distance within the flavonolato chelate ring is similar in all three complexes (**1·2CH$_2$Cl$_2$**: 1.458(4) Å; **3·CH$_3$CN**: 1.439(3) Å; **4·CHCl$_3$**; 1.460(4) Å) and is elongated relative to that found in the free flavonol (1.363(4) Å) [32]. Overall, the bond lengths within the flavonolato ligands of this series of complexes are only minimally affected by the nature of the supporting chelate ligand.

In **4·CHCl$_3$**, hydrogen bonds are found between the two secondary amine NH units of the bnpapa chelate ligand and O(1) of the coordinated flavonolato ligand. The heteroatom distances (2.93 and 3.01 Å) and corresponding N–H···O angles (136.5° and 155.2°) associated with these interactions suggest that these are moderate hydrogen bonds with individual energies of 4–14 kcal mol^{-1} [33].

3.2.4. Spectroscopic characterization. Powdered samples of **3** and **4** were characterized by solid-state IR spectroscopy, and solutions of these complexes were examined using ^{1}H NMR, mass spectrometry, and absorption and emission spectroscopy.

3.2.4.1. *Infrared spectra.* The solid-state FTIR spectra of **1**, **3**, and **4** contain a $\nu_{C=O}$ vibration at ~1550–1560 cm^{-1} for the coordinated ketone moiety, as well as vibrations for the perchlorate counterion. For **4**, a broad vibration at ~3300 cm^{-1} is consistent with the presence of the secondary amine appendages and their involvement in hydrogen-bonding interactions with the coordinated flavonolato ligand.

3.2.4.2. *^{1}H NMR.* Complex **1** exhibits a ^{1}H NMR spectrum with the appropriate number of signals for C_s symmetry in CD$_3$CN (figure S1, see online supplemental material at http://dx.doi.org/10.1080/00958972.2014.977272). This is consistent with coordination of all of the nitrogen donors of the 6-Ph$_2$TPA ligand in the solution structure of the complex. Complex **3** exhibits broadened ^{1}H NMR signals suggestive of fluxional behavior when dissolved in CD$_3$CN (figure S2) or CD$_2$Cl$_2$ [figure S3(a)] at 25 °C. The broadened benzylic methylene

resonance at ~4.4 ppm suggests that the fluxionality could involve dissociation and reassociation of pyridyl donors (figure S3). This type of behavior has been previously identified in d^{10} Cu(I) complexes of TPA [34]. Cooling of a CD_2Cl_2 solution of **3** from 25 °C to −53.5 °C [figure S3(a)–(h)] produced a sharpening of some of the resonances that was reversible upon returning the sample to room temperature. Further evaluation of the ^{1}H NMR properties of **3** are underway. Complex **4** exhibits ^{1}H NMR features (figure S5) consistent with the cationic portion having C_s symmetry.

3.2.4.3. *Mass spectrometry.* Complexes **3** and **4** were evaluated by MALDI mass spectrometry (figures S4 and S6, respectively). Each exhibits an isotopic cluster molecular ion that is consistent with the proposed cationic formulation.

3.2.4.4. *Absorption and emission spectra in CH_3CN and 1 : 1 H_2O : DMSO.* Free 3-hydroxyflavone (3-HflH) exhibits absorption bands at 304 and 343 nm, respectively, when dissolved in methanol [35, 36]. The lower energy feature (Band I) is assigned to a $\pi \rightarrow \pi^*$ HOMO to LUMO transition, while the higher energy Band II corresponds to a HOMO-1 to LUMO transition. The absorption spectra of **3** and **4** in CH_3CN are shown in figure 3. The Band I absorption feature for **1**, **3,** and **4** is red-shifted relative to the neutral flavonol, with the degree of shift depending on the nature of the supporting chelate ligand. Specifically, the most red-shifted Band I absorption is found for the 6-Ph_2TPA-ligated complex **1** (λ_{max} = 420 nm (21,000 M^{-1} cm^{-1})) [16], followed by those of **3** (λ_{max} = 415 nm (16,500 M^{-1} cm^{-1})) and **4** (λ_{max} = 401 nm (16,500 M^{-1} cm^{-1})). In 1 : 1 DMSO : H_2O, the TPA-supported complex **3** exhibits spectral changes consistent with protonation of the coordinated flavonolato ligand and displacement from the Zn(II) center [figure 3(a)]. A new absorption feature at ~350 nm is consistent with the presence of free 3-hydroxyflavone [figure 3(a)]. The UV–vis absorption spectrum of **4** in 1 : 1 DMSO : H_2O is similar to that found in CH_3CN [figure 3(b)] albeit with significantly lower molar absorptivity values.

Excitation into the ~400–415 nm absorption maximum of **3** and **4** dissolved in CH_3CN (5×10^{-5} M) produced the emission spectra shown in figure 4. Compound **3** exhibits a

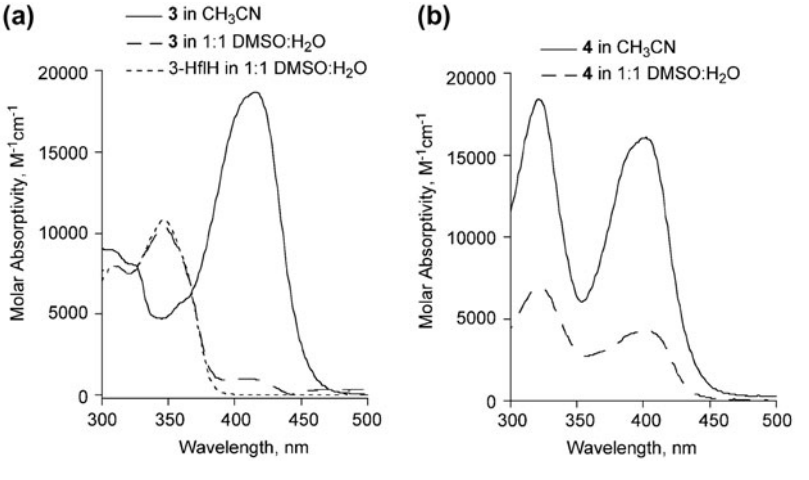

Figure 3. (a) Absorption spectra of **3** in CH_3CN and 1 : 1 DMSO : H_2O and the absorption spectrum of 3-hydroxyflavone in 1 : 1 DMSO : H_2O. (b) Absorption spectra of **4** in CH_3CN and 1 : 1 DMSO : H_2O.

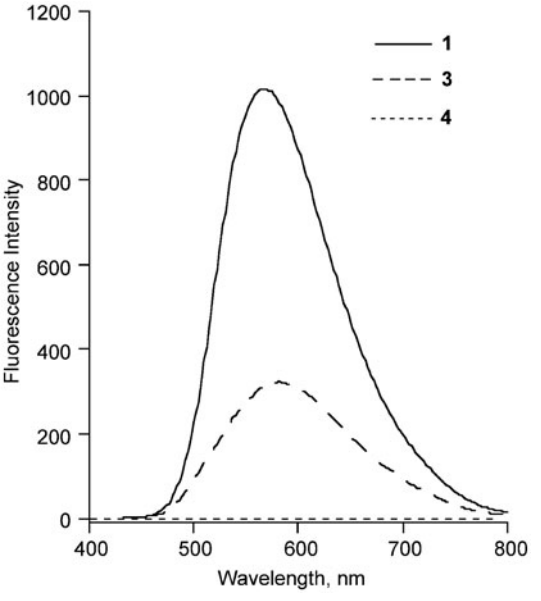

Figure 4. Fluorescence emission spectra of **1**, **3**, and **4** in CH_3CN. All spectra were obtained with λ_{ex} at the absorption maximum at ~400–420 nm.

similar Stokes shift (~72 nm) to that found for **1**, but with an overall lower intensity fluorescent emission. Essentially, no fluorescent emission is observed for **4** upon excitation at its absorption maximum (401 nm). Thus, the fluorescence intensity decreases in the order of **1** > **3** > **4** in CH_3CN. We propose that this difference relates to the microenvironment surrounding the coordinated flavonolato ligand. Specifically, the presence of the phenyl appendages in the 6-Ph_2TPA chelate in **1** results in the flavonolato ligand being positioned in a hydrophobic microenvironment. This motif limits solvent access to the flavonolato ligand relative to that in **3** thereby reducing collisional quenching. That being said, in 1 : 1 H_2O : DMSO, the emission of **1** decreases in intensity relative to that found in CH_3CN [figure 1(b)], suggesting that there is some solvent access to the flavonolato moiety. For complex **4**, the presence of the rigid intramolecular hydrogen-bond donors, which may undergo excited state lengthening or shortening, results in significant fluorescence quenching [37].

3.3. *Visible light-induced reactivity of 3 and 4*

As **3** undergoes reaction in 1 : 1 H_2O : DMSO to produce free 3-hydroxyflavone, we have only examined the visible light-induced CO-release reactivity of this compound in aerobic CH_3CN using 419 nm irradiation. Complex **4** was also examined in aerobic CH_3CN and was found to exhibit such low photochemical efficiency (vide infra) that further studies in 1 : 1 H_2O : DMSO were not performed. Each reaction mixture was irradiated until judged to be complete by the disappearance of the ~400–415-nm absorption band.

3.3.1. Product Identification. GC headspace gas analysis, ^{1}H NMR, IR, and mass spectrometry were used to characterize the products generated upon photoirradiation of **3** and **4** in CH_3CN at 419 nm. For each complex, the photoreaction resulted in the formation of one equivalent of CO (table 1) as well as a [(L)Zn(*O*-bs)]ClO_4 complex (TPA: **5**; bnpapa: **6**). The latter complexes were identified by their ^{1}H NMR spectral features (S7 and S10), molecular ions in MALDI mass spectral experiments (figures S8, S9, S11, and S12), and by their characteristic $\nu_{C=O}$ ester vibration at 1740–1770 cm^{-1} for the *O*-benzoylsalicylato ligand. Quantitative ^{18}O incorporation from $^{18}O_2$ for the reactions of **3** and **4** provides conclusive evidence for a dioxygenase-type reaction. Appropriate dark and anaerobic control reactions demonstrate that the observed reactions for **3** and **4** are O_2-dependent photoinduced processes.

3.3.2. Reaction Quantum Yields. The quantum yields for the visible light-induced CO-release reactions of **3** and **4** in CH_3CN are shown in table 1. The structure of the supporting chelate ligand has a significant effect on the photochemical efficiency of the CO-release reactions, with the quantum yield for **1** being twofold higher than that of **3**, and both of these values being >20-fold higher than the quantum yield for the reaction of **4**. These results demonstrate that positioning a zinc flavonolato moiety within a rigid hydrogen-bond donor environment significantly stabilizes the compound with respect to light-induced reactivity.

4. Conclusions

In the studies outlined herein, we have examined the aqueous, visible light-induced CO-release reactivity properties of **1**. The results indicate that this complex is stable in an aqueous, aerobic environment in the dark, but will exhibit quantitative, visible light-induced CO-release to generate a single zinc-containing product. The quantum yield for CO-release in 1 : 1 H_2O : DMSO is a factor of two lower than that observed in organic solvent.

We have also examined how the supporting chelate ligand influences the aqueous stability and visible light-induced CO-release reactivity of zinc flavonolato species. We were particularly interested in examining the influence of the aryl appendages of the 6-Ph_2TPA ligand in **1** as it is well known that the photochemical reactivity of organic and inorganic molecules can be modulated via encapsulation within a confined microenvironment such as a cyclodextrin cavity, hydrogen-bonded capsules, or hollow molecular structure [38, 39]. Our results demonstrate that the secondary environment introduced by the tetradentate chelate ligand influences the chemistry of zinc flavonolato complexes in multiple ways. First, the presence of the hydrophobic microenvironment in **1** stabilizes the zinc flavonolato moiety with respect to water and differentiates the chemistry of **1** from that of **3** in aqueous DMSO solution. The observation of flavonol displacement from **3** in water is noteworthy not only to this study but also to investigations being performed in other laboratories wherein simple zinc flavonolato species such as [Zn(3-Hfl)(acetate)] are being evaluated in aqueous media for their antidiabetic and DNA binding properties [40–42]. Second, the lower quantum yields observed for photoinduced CO-release from **3** and **4** in CH_3CN relative to **1** is likely a consequence of the enhanced accessibility of solvent to the flavonolato moiety and/or secondary hydrogen bonding. These interactions offer additional pathways

for non-radiative decay thus leading to the observed excited state quenching and less efficient CO-release processes relative to **1**.

Overall, these investigations revealed that the presence of a hydrophobic microenvironment is important toward providing aqueous stability and maximizing the photochemical efficiency of the CO-release reaction of a zinc flavonolato moiety. Therefore, if zinc flavonolato species are to be advanced for use as photoinduced CO-release agents in biological systems, careful consideration will need to be given to the supporting microenvironment within the compound.

Supplementary material

^{1}H NMR data for **1** and **3–6**; MALDI-MS data for **3–6**. CCDC 1006159 and 1006160 contain the supplementary crystallographic data for this paper. This data can be obtained free of charge from The Cambridge Crystallographic Data Center via www.ccdc.cam.ac.uk/data_request/cif.

Funding

This work was supported by the National Science Foundation under grants [grant number CHE-0094066], [grant number CHE-1301092].

References

[1] U. Schatzschneider. *Br. J. Pharmacol.*, (2014). doi:10.1111/bph.12688.
[2] S. García-Gallego, G.J.L. Bernardes. *Angew. Chem. Int. Ed. Engl.*, **53**, 9712–9721 (2014). doi:10.1002/anie.201311225.
[3] F. Zobi. *Future Med. Chem.*, **5**, 175–188 (2013).
[4] C.C. Ramão, W.A. Blättler, J.D. Seixas, G.J.L. Bernardes. *Chem. Soc. Rev.*, **41**, 3571–3583 (2012).
[5] B.E. Mann. *Organometallics*, **31**, 5728–5735 (2012).
[6] R. Motterlini, L.E. Otterbein. *Nat. Rev. Drug Discov.*, **9**, 728–743 (2010).
[7] B.E. Mann. *Top. Organomet. Chem.*, **32**, 247–285 (2010).
[8] M.A. Gonzales, P.K. Mascharak. *J. Inorg. Biochem.*, **133**, 127–135 (2014).
[9] I. Chakraborty, S.J. Carrington, P.K. Mascharak. *ChemMedChem.*, **9**, 1266–1274 (2014).
[10] I. Chakraborty, S.J. Carrington, P.K. Mascharak. *Acc. Chem. Res.*, **47**, 2603–2611 (2014).
[11] R.D. Rimmer, A.E. Pierri, P.C. Ford. *Coord. Chem. Rev.*, **256**, 1509–1519 (2012).
[12] U. Schatzschneider. *Inorg. Chim. Acta*, **374**, 19–23 (2011).
[13] D. Crespy, K. Landfester, U.S. Schubert, A. Schiller. *Chem. Commun.*, **46**, 6651–6662 (2010).
[14] S. Fetzner. *Appl. Environ. Microbiol.*, **78**, 2505–2514 (2012).
[15] K. Grubel, B.J. Laughlin, T.R. Maltais, R.C. Smith, A.M. Arif, L.M. Berreau. *Chem. Commun.*, **47**, 10431–10433 (2011).
[16] K. Grubel, A.R. Marts, S.M. Greer, D.L. Tierney, C.J. Allpress, S.N. Anderson, B.J. Laughlin, R.C. Smith, A.M. Arif, L.M. Berreau. *Eur. J. Inorg. Chem.*, 4750–4757 (2012).
[17] W.L.F. Armarego, D.D. Perrin. *Purification of Laboratory Chemicals*, 4th Edn, Butterworth-Heinemann, Boston, MA (1996).
[18] J.W. Canary, Y. Wang, R. Roy, L. Que, Jr., H. Miyake. *Inorg. Synth.*, **32**, 70–75 (1998).
[19] E. Szajna-Fuller, B.M. Chambers, A.M. Arif, L.M. Berreau. *Inorg. Chem.*, **46**, 5486–5498 (2007).
[20] K. Grubel, K. Rudzka, A.M. Arif, K.L. Klotz, J.A. Halfen, L.M. Berreau. *Inorg. Chem.*, **49**, 82–96 (2010).
[21] C.G. Hatchard, C.A. Parker. *Proc. R. Soc. London A*, **235**, 518–536 (1956).
[22] H.J. Kuhn, S.E. Braslavsky, R. Schmidt. *Pure Appl. Chem.*, **76**, 2105–2146 (2004).
[23] K. Grubel, S.L. Saraf, S.N. Anderson, B.J. Laughlin, R.C. Smith, A.M. Arif, L.M. Berreau. *Inorg. Chim. Acta*, **407**, 91–97 (2013).
[24] W.C. Wolsey. *J. Chem. Educ.*, **50**, A335–A337 (1973).

[25] E. Szajna, M.M. Makowska-Grzyska, C.C. Wasden, A.M. Arif, L.M. Berreau. *Inorg. Chem.*, **44**, 7595–7605 (2005).
[26] Z. Otwinowski, W. Minor. *Methods Enzymol.*, **276**, 307–326 (1997).
[27] G.M. Sheldrick. *SHELX97, Programs for Crystal Structure Analysis (Release 97-2)*, University of Göttingen, Germany (1997).
[28] A.W. Addison, T.N. Rao, J. Reedijk, J. van Rijn, G.C. Verschoor. *J. Chem. Soc., Dalton Trans.*, 1349–1356 (1984).
[29] É. Balogh-Hergovich, J. Kaizer, G. Speier, G. Huttner, P. Rutsch. *Acta Crystallogr., Sect. C: Cryst. Struct. Commun.*, 55, 557–558 (1999).
[30] T.A. Annan, C. Peppe, D.G. Tuck. *Can. J. Chem.*, **68**, 423–430 (1990).
[31] J. Kaizer, A. Kupán, J. Pap, G. Speier, M. Réglier, G. Michel. *Z. Kristallogr. – New Cryst. Struct.*, **215**, 571–572 (2000).
[32] M.C. Etter, Z. Urbańczyk-Lipkowska, S. Baer, P.F. Barbara. *J. Mol. Struct.*, **144**, 155–167 (1986).
[33] G.A. Jeffrey. *An Introduction to Hydrogen Bonding*, Oxford University Press, New York, NY (1997).
[34] Z. Tyeklar, R.R. Jacobson, N. Wei, N.N. Murthy, J. Zubieta, K.D. Karlin. *J. Am. Chem. Soc.*, **115**, 2677–2689 (1993).
[35] L. Jurd, T.A. Geissman. *J. Org. Chem.*, **21**, 1395–1401 (1956).
[36] S. Protti, A. Mezzetti, C. Lapouge, J.-P. Cornard. *Photochem. Photobiol. Sci.*, **7**, 109–119 (2008).
[37] N. Barman, D. Singha, K. Sahu. *J. Phys. Chem. A*, **117**, 3945–3953 (2013).
[38] V. Ramamurthy, D.F. Eaton. *Acc. Chem. Res.*, **21**, 300–306 (1988).
[39] O.B. Berryman, H. Dube, J. Rebek Jr. *Isr. J. Chem.*, **51**, 700–709 (2011).
[40] K. Vijayaraghavan, S. Iyyam Pillai, S.P. Subramanian. *Eur. J. Pharmacol.*, **680**, 122–129 (2012).
[41] K. Vijayaraghavan, S. Iyyampillai, S.P. Subramanian. *J. Diabetes*, **5**, 149–156 (2013).
[42] S. Iyyam Pillai, K. Vijayaraghavan, S. Subramanian. *Der Pharma Chemica*, **6**, 379–389 (2014).